

Engineering & Laboratory Notes

Simple Fast Light Detector Device Based on a 1P28 Photomultiplier Tube

A.R. Libertun, M.C. Marconi, and G. Sánchez, Laboratorio de Electrónica Cuántica, Departamento de Física, Universidad de Buenos Aires, Ciudad Universitaria, Buenos Aires, Argentina.

Abstract

A simple implementation of the stroboscopic optical boxcar technique for determining intensity profiles of repetitive nanoseconds light pulses is presented. The device, implemented with standard components and a 1P28 photomultiplier tube, can be used for fluorescence decay measurements with subnanosecond time resolution.

The time profile measurement of short light pulses usually requires advanced detectors, such as fast photomultipliers based on microchannel plates, or fast photodiodes, which should be used with large bandwidth oscilloscopes. We present here an alternative device based on the stroboscopic optical boxcar (SOB) technique.¹ Using a 1P28 phototube and a simple HV switch circuit, it is possible to get the time profile of repetitive light pulses with subnanosecond resolution.

In the SOB technique, as in any stroboscopic technique, the signal is obtained recording the intensity measured during a very narrow temporal window and the time delay at which the measurement was made. Thus, this technique requires a synchronous trigger signal with an adjustable delay and a detector with a gate time shorter than the characteristic time of the signal to be measured.

For this device we used a PMT with a polarization circuit modified to generate the required gate effect. The polarization of the dynodes is produced by an electrical pulse of steep negative slope traveling along a transmission line that interconnects the PMT's dynodes. The transmission line introduces a time delay on the arrival of the electrical pulse to each dynode and produces a transient interdynode voltage difference. The interdynode voltage varies with time depending on the position of the polarizing pulse in the transmission line. Initially, when the pulse has only arrived to the photocatode, the voltage between the photocatode and the first dynode increases with the rate of the polarizing pulse. Then, if the transit time of the HV pulse traveling between dynodes (t_t) is shorter than the pulse rise time (T), the edge of the pulse will reach the first dynode while the voltage at the photocatode is still increasing. As long as the pulse voltage augments in both electrodes simultaneously, the accelerating voltage will remain constant at its maximum value Et_t/T , where E is the polarizing pulse peak value. Finally, when the pulse at the photocatode reaches its peak value, the accelerating voltage starts to decrease and eventually becomes null. The same cycle occurs at the subsequent stages, but with a time shift corresponding to a pulse transit time between stages.

The transient interdynode voltage, traveling through

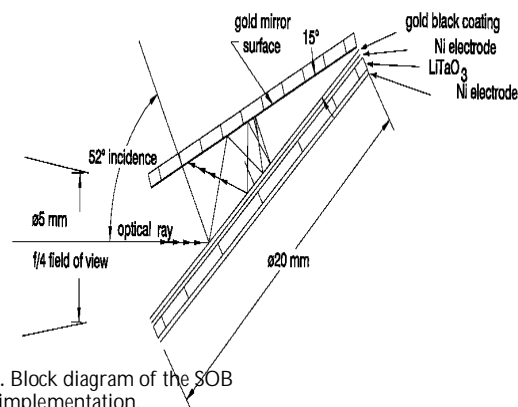


FIGURE 1. Block diagram of the SOB method implementation.

the dynodes, accelerates the photoelectrons from one dynode to the other and generates simultaneously a strobe effect on the photoelectrons. Electrons with flying times (t_f) similar to the electrical pulse traveling time, will find a favorable polarization sequence and be the main contributors to the final signal. Those electrons with t_f different from t_t make no contribution to the final signal because they do not find the appropriate polarization in the amplification stages to be accelerated from one dynode to the other.

The flying time of the electrons between dynodes depends on the interdynode voltage, which is a function of the pulse peak value, its rise time, and the interdynode travel time. To evaluate the effective duration of the detection window (τ_n) produced by the HV pulse in the PMT, we considered that the successive dynodes are active only during the time of maximum voltage difference. With this consideration τ_n is:

$$\tau_n = \begin{cases} T - (n-1)t_f + (n-2)t_t & t_t \leq t_f \\ T + (n-1)t_f - nt_t & t_t > t_f \end{cases}$$

where T is the HV pulse rise time, n is the number of dynodes, t_f is the flying time of the electrons between dynodes, and t_t is the travel time of the HV pulse between dynodes.

The duration of the detection window τ_n increases for transit times shorter than the flying time and decreases for transit times longer than the flying time. It reaches the max-

In this section . . .

Simple Fast Light Detector Device Based on a 1P28 Photomultiplier Tube

Pyroelectric Trap Detector for Spectral Responsivity Measurements

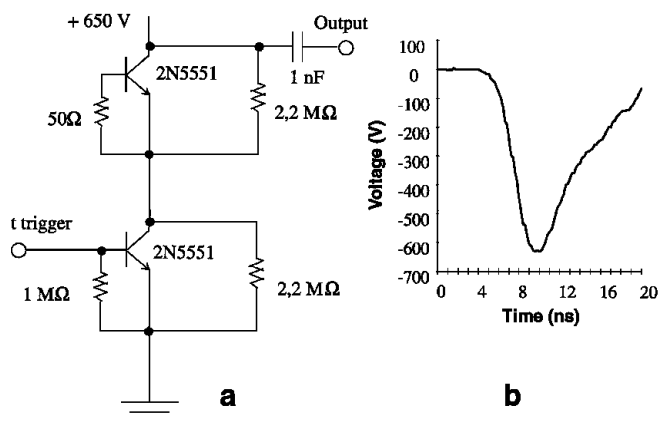


FIG. 2. (a) High voltage pulse generator circuit (HV PGC). (b) HV output pulse generated with the PGC (-650 V peak, -192 V/nsec slope).

imum value when both times are equal ($t_t = t_p$), that is when the polarization pulse and the photoelectrons travel synchronously along the dynodes.

Figure 1 shows a block diagram of the method implemented for fluorescence lifetime measurement. The laser provides the excitation pulse and also generates the master trigger signal for the measurement process. The master trigger fires the pulse generator circuit (PGC), which provides the HV pulse to be injected in the interdynode delay line (IDL). The delay between dynodes introduced by the IDL can be adjusted to get the desired gate duration in the PMT.

To start the measurement, the delay is set to a value so that the HV pulse reaches the PMT just before the light pulse arrives at it. The measurement process consists of recording the output signal in the PMT simultaneously with the time delay between the polarization pulse and the excitation. Varying the time delay, the signal under study is completely scanned.

The curve obtained plotting the PMT output as a function of the time delay corresponds to the convolution of the light pulse profile with the profile of the temporal window of the strobed detector. The temporal profile of the light pulse can be retrieved from this curve.

Figure 2a is a schematic of the HV PGC we have used for this device. It is a one stage avalanche transistor circuit^{2,3} that provides a pulse of great stability and low jitter. In this circuit the transistors act as very fast switches that discharge in less than 3 nsec the capacitor charged at 650 V. The 192 V/nsec slope HV pulse provided by the circuit (see Fig. 2b) presented a measured jitter of less than 100 psec and no appreciable peak voltage variation.

We have determined the interdynode delay of the IDL (see Fig. 3) based on the corresponding τ_n function for a 1P28 PMT ($n = 9$) polarized with a 424V, 2.2 nsec rise time pulse. We tested the device adjusting the effective gate time duration to its largest value—800 psec—setting a delay of a 1.45 nsec. The transmission line of the IDL was made using a 50 Ω coaxial cable.

The RC in the anode provides an integration network to obtain a constant output level proportional to the light signal at this particular delay time. This constant voltage level can be measured with a slow time response voltmeter, thereby avoiding the necessity of large bandwidth oscilloscopes.

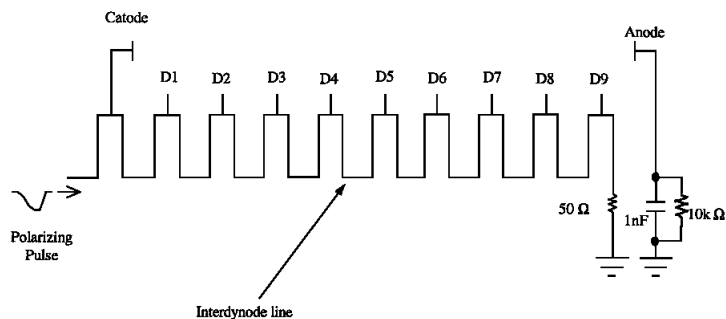


FIGURE 3. Interdynode delay line (IDL) for a 1P28 PMT. The HV pulse travels along the line with transit time t_t between dynodes.

The 1P28 was mounted on the same circuit board as the HV pulser circuit. A compact layout was used to achieve fast pulses avoiding parasitic inductances. The 50 Ω lines used as IDL were included in the same board, keeping a very compact configuration.

We tested the system with the output pulse of a Q-switched Nd:YAG laser. This pulse presents a three-peak structure, each with a 3 nsec FWHM. Figure 4 shows the experimental data obtained for SOB's rise flank of the pulse compared with the signal acquired using an ultrafast photodiode and a digital oscilloscope in sampling mode, with an overall time resolution of 200 psec. The data obtained with the SOB detector follows the shape of the laser pulse showing the internal structure clearly.

In conclusion, we found that the stroboscopic optical boxcar technique is a simple and inexpensive alternative to obtain subnanosecond time resolution. This method makes use of low-cost and "off the shelf" electronic components. It does not require fast photomultiplier tubes or wide bandwidth oscilloscopes to determine temporal profiles of repetitive nanoseconds light pulses. It is particularly useful for high repetition rate light signals. The HV pulser we have developed based on an avalanche configuration shows high stability, negligible jitter, and good performance.

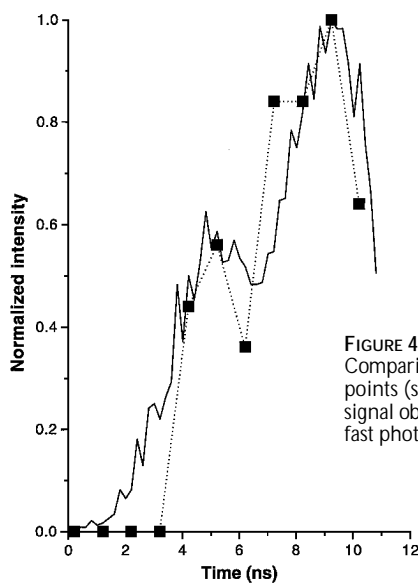


FIGURE 4. Experimental results: Comparison of the SOB data points (solid squares) with the signal obtained with an ultrafast photodiode (solid line).

Acknowledgments

We acknowledge the support from Universidad de Buenos Aires (Project EX285).

References

1. D.R. James *et al.*, "Stroboscopic optical boxcar technique for the determination of fluorescence lifetimes,"

Rev. Sci. Instrum. **63** (2), 1710 (1992).

2. I. Matsushima *et al.*, "Single pulse switchout system for a passively mode-locked Q-switched Nd:YAG laser," Rev. Sci. Instrum. **52**, 1860 (1981).

3. W.M. Henebry, "Avalanche transistor circuits," Rev. Sci. Instrum. **32**, 1198 (1961).

Pyroelectric Trap Detector for Spectral Responsivity Measurements

J.H. Lehman, National Institute of Standards and Technology, Sources and Detectors Group, Boulder, Colo.

Abstract

We have designed and built a pyroelectric optical detector for use as a transfer standard for the calibration of optical power meters. The pyroelectric element is made from lithium tantalate (LiTaO_3). Gold black is used as the optical absorber in a multiple reflection wedge-shaped trap structure, with a 5-mm diameter input aperture and an f/4 field-of-view. The detector's spatial responsivity varies less than 1%. The responsivity as a function of wavelength varies less than 1% over a range from 0.45–1.55 μm and less than 4% from 1.55–10.6 μm . The measured noise equivalent power (NEP) is $5 \times 10^{-8} \text{ W/Hz}^{1/2}$. For this wavelength range and detector area, the measured NEP and spatial uniformity represents a significant improvement over comparable predecessors.

Pyroelectric detectors that are designed for radiometric applications typically demonstrate spatial uniformity variations of $\pm 2\%$, NEP ranging from $10^{-7} \text{ W/Hz}^{1/2}$ (no window) to less than $10^{-8} \text{ W/Hz}^{1/2}$ (small area, sealed container with a window), and a wavelength sensitivity ranging from the visible to beyond 10 μm . Despite years of development and commercial success, these numbers do not represent the theoretical performance limits for pyroelectric detectors. Although we have not yet reached the theoretical limits of performance, we have achieved a design compromise that optimizes those detector properties that are important for high accuracy spectral responsivity and absolute power measurements.

Detector design considerations

Our first design compromise forced a choice between detector sensitivity, spatial uniformity, and the practical matter of fabricating the pyroelectric detector element. The pyroelectric element chosen for this design is a 20-mm diameter, 250- μm thick, LiTaO_3 electret that is poled perpendicular to the faces. The faces are polished to a specification of less than 40/20 scratch/dig and parallelism of 2" or less. The LiTaO_3 electret is coated on each face with nickel electrodes that are 25-nm thick.

If a pyroelectric detector is constructed using an electret that is perfectly flat and has a perfectly uniform thickness, then the responsivity over the entire area of the detector will be uniform. Since the pyroelectric current output is inversely proportional to electret thickness, thinner electrets will produce higher electrical currents for a given optical input.¹ Although we can obtain a greater current responsivity using a thinner electret, a geometrically flat and uni-

formly thick electret becomes more difficult and expensive to fabricate as the thickness decreases.

In addition to high optical sensitivity and uniform spectral responsivity, a detector with a broad and uniform spectral responsivity is desired. We achieved this by depositing gold black on one side of the nickel-coated electret and placing it into a wedge-shaped optical trap structure. The goal of this trap structure is for all the radiation passing through the detector aperture to be absorbed by the gold black coating. A cross section of the wedge-trap is shown in Figure 1. The trap has a 5-mm diameter aperture and an f/4 field-of-view. Light entering the trap intersects the electret at an incidence angle of 52° . A gold mirror, situated opposite the electret at an angle of 15° , reflects radiation not absorbed by the pyroelectric element back onto the absorber.

The optical trap geometry is based on the input radiation achieving three specular reflections from the gold mirror and up to four specular reflections from the gold black. Published data shows that gold black coatings diffusely reflect less than 1% of incident radiation over a spectral range from the ultraviolet to 15 μm .^{2, 3} We have been unable to deposit a gold black coating that is highly absorbing for wavelengths beyond 2.5 μm onto LiTaO_3 . Our measurements show that, from 2.5 μm to 10 μm , the reflection gradually becomes more nearly specular and increases to as much as 15%. At shorter wavelengths such as 633 nm, reflectance from the gold black coating is diffuse and small.⁴ If we assume that the gold mirror is a perfect reflector and that the gold black coating is specular, the gold black coating may have a coefficient of absorptance as low as 85% and still achieve a total absorptance greater than 99.5%. Overall, we expect the detector's relative spectral responsivity to decrease from 99.9% at 2.5 μm to 99.5% at 10 μm because the gold mirror is not a perfect reflector and will absorb as much as 0.5% of the radiation reflected by the gold black coating at wavelengths beyond 2.5 μm .

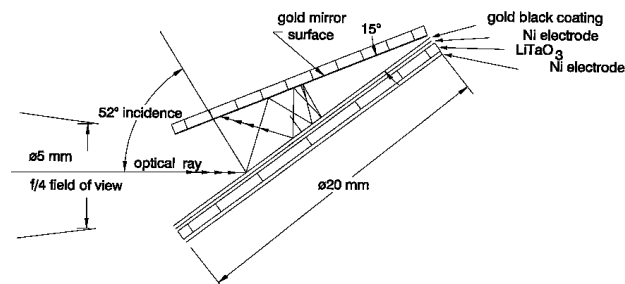


FIGURE 1. Wedge-trap configuration with ray tracing lines inside the trap cavity.

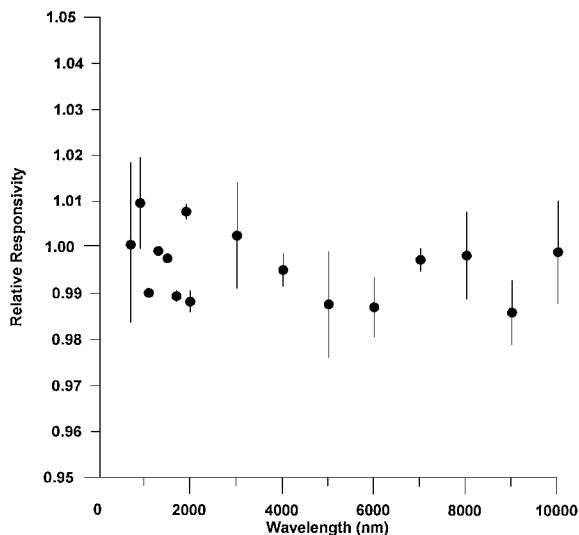


FIGURE 2. Relative spectral responsivity of wedge-trap detector.

Measurements

To measure spatial uniformity, the collimated light from a laser diode operating at a wavelength of 674 nm was used as a probe and focused at the aperture plane to a spot diameter less than 300 μm . As the laser probe beam was scanned across the detector's aperture at equally spaced, 250 μm intervals, the detector signal was sampled and recorded. Repeated measurements show that the detector responsivity is within $\pm 0.5\%$ of the average value and has a standard deviation of less than 0.15%. Using light at normal incidence, we have also measured comparable spatial uniformity for this type of LiTaO_3 pyroelectric detector not mounted in a trap configuration.

Next we compared the spectral responsivity of the wedge-trap LiTaO_3 pyroelectric detector to a hemispherical trap polyvinylidene fluoride (PVF2) pyroelectric detector.⁴ Data was obtained at several wavelengths from 674 nm through 10.6 μm using various light sources and a sodium chloride prism monochromator having 20-nm resolution. Figure 2 shows the spectral responsivity of the wedge-trap relative to the hemispherical trap. The data was normalized to 1 at 674 nm, and the error bars indicate the standard deviation of data acquired for each wavelength. The standard deviation varies because the optical efficiency of the measurement system (*i.e.*, prisms, mirrors, lamps) varies as a function of wavelength and appears relatively large because of the limited sensitivity of the hemispherical trap. The results indicate that the spectral responsivity variation of the wedge-trap detector is less than 2% over this wavelength region. The accuracy of the measurement system is limited by the monochromator performance and by the accuracy of the hemispherical trap, which together limit the uncertainty to $\pm 2\%$.

We have also compared the wedge-trap detector to a NIST reference laser calorimeter and a commercial electrically calibrated pyroelectric radiometer (ECPR). Using laser sources with wavelengths ranging from 488–1550 nm, we have found agreement to be within 1%, with an estimated measurement uncertainty of $\pm 0.5\%$.⁵

The pyroelectric detector's sensitivity was measured in the laboratory by modulating the optical power input and observing the electrical output using a current preamplifier and a lock-in amplifier. The optical power input ranged

from a few microwatts to a few hundred microwatts. We have applied 1 W without damage to the pyroelectric crystal. However, the damage threshold for the gold black coating places an upper limit of 0.2 W/cm^2 on the allowable irradiance. The measured absolute detector responsivity was about 3×10^{-8} A/W.

The measured NEP of the wedge-trap detector was 5×10^{-8} $\text{W}/\text{Hz}^{1/2}$. Using the input noise current of 0.5×10^{-15} $\text{A}/\text{Hz}^{1/2}$, specified by the amplifier manufacturer for an amplifier feedback resistance of 1×10^{12} Ω , we calculated the expected NEP to be 1.7×10^{-8} $\text{W}/\text{Hz}^{1/2}$. Therefore, the measured 5×10^{-8} $\text{W}/\text{Hz}^{1/2}$ is approaching the limit imposed by the best commercially available current amplifiers. The value of the measured NEP is nearly one tenth that of our existing reference pyroelectric detectors used for relative spectral responsivity.⁴

Conclusion

The performance of the present device represents a factor of 5 to 10 improvement in spatial uniformity over other large area pyroelectric detectors that have a broad and uniform spectral responsivity from 450 nm to 10 μm . In addition, the NEP represents a factor of 10 improvement for pyroelectric detectors we have made with comparable active area, spatial uniformity, and spectral responsivity. The goal of our future work will be to reduce the NEP below 5×10^{-8} $\text{W}/\text{Hz}^{1/2}$ while maintaining the spatial and spectral uniformity over a larger detector area. In addition, the pyroelectric wedge-trap detector will be useful for improving our spectral responsivity measurement system capability.

Acknowledgments

The design of the optical trap was done in collaboration with Robert J. Phelan Jr., Boulder Metric, Inc., whose advice and many discussions about pyroelectric detectors I appreciate. I also thank Igor Vayshenker and Iris Tobias for making various calibration measurements.

References

1. R.L. Peterson *et al.*, "Analysis of response of pyroelectric optical detectors," *J. Appl. Phys.* **45** (8), (1974).
2. D.J. Advena *et al.*, "Deposition and characterization of far-infrared absorbing gold black films," *Appl. Opt.* **32**, (7), (1993).
3. W.R. Blevin and W.J. Brown, "Black coatings for absolute radiometers," *Metrologia* **2** (4), (1966).
4. G.W. Day *et al.*, "Spectral reference detector for the visible to 12- μm region; convenient, spectrally flat," *Appl. Opt.* **15** (7), (1976).
5. E.D. West *et al.*, "A reference calorimeter for laser energy measurements," *J. Res. Nat. Bur. Stand. (U.S.)*, **76A** (1), 13 (1972).

Engineering & Laboratory Notes

EDITOR

ROBERT R. SHANNON, *University of Arizona*

STAFF

JENNIFER RICE, *Production Editor*
ALEXINE MOORE, *Manuscript Coordinator*
FRANCES GREENE, *Production Assistant*

Please mail manuscripts to
Engineering & Laboratory Notes
c/o Optics & Photonics News, OSA
2010 Massachusetts Ave., N.W.
Washington, D.C. 20036-1023

For questions on manuscript submission, status, or author guidelines, contact Frances Greene, 202/416-1423; fgreen@osa.org.